THE JOURNAL OF BIOLOGICAL CHEMISTRY VOL. 286, NO. 21, pp. 18492–18504, May 27, 2011

Rap1-GTP-interacting Adaptor Molecule (RIAM) Protein Controls Invasion and Growth of Melanoma Cells*[S]

Received for publication, September 29, 2010, and in revised form, March 25, 2011 Published, JBC Papers in Press, March 26, 2011, DOI 10.1074/jbc.M110.189811

Pablo Hernández-Varas[‡1], Georgina P. Coló[‡1], Ruben A. Bartolomé[‡], Andrew Paterson[§], Iria Medraño-Fernández[¶], Nohemí Arellano-Sánchez[‡], Carlos Cabañas[‖], Paloma Sánchez-Mateos[**], Esther M. Lafuente[¶], Vassiliki A. Boussiotis[‡‡], Staffan Strömblad[§], and Joaquin Teixidó[‡2]

From the [‡]Department of Cellular and Molecular Medicine, Centro de Investigaciones Biológicas, 28040 Madrid, Spain, the [§]Center for Biosciences, Department of Biosciences and Nutrition, Karolinska Institutet, SE-141 83 Huddinge, Sweden, the [¶]Facultad de Medicina, Department of Microbiology and Instituto de Investigación Hospital 12 de Octubre, Universidad Complutense de Madrid, 28041 Madrid, Spain, the [‖]Centro de Biología Molecular, 28049 Madrid, Spain, the [**]Servicio de Inmuno-Oncología, Hospital Universitario Gregorio Marañón, 28007 Madrid, Spain, and the [‡‡]Division of Hematology and Oncology, Department of Medicine, Harvard Medical School, Boston, Massachusetts 02115

The Mig-10/RIAM/lamellipodin (MRL) family member Rap1-GTP-interacting adaptor molecule (RIAM) interacts with active Rap1, a small GTPase that is frequently activated in tumors such as melanoma and prostate cancer. We show here that RIAM is expressed in metastatic human melanoma cells and that both RIAM and Rap1 are required for BLM melanoma cell invasion. RIAM silencing in melanoma cells led to inhibition of tumor growth and to delayed metastasis in a severe combined immunodeficiency xenograft model. Defective invasion of RIAM-silenced melanoma cells arose from impairment in persistent cell migration directionality, which was associated with deficient activation of a Vav2-RhoA-ROCK-myosin light chain pathway. Expression of constitutively active Vav2 and RhoA in cells depleted for RIAM partially rescued their invasion, indicating that Vav2 and RhoA mediate RIAM function. These results suggest that inhibition of cell invasion in RIAM-silenced melanoma cells is likely based on altered cell contractility and cell polarization. Furthermore, we show that RIAM depletion reduces β1 integrin-dependent melanoma cell adhesion, which correlates with decreased activation of both Erk1/2 MAPK and phosphatidylinositol 3-kinase, two central molecules controlling cell growth and cell survival. In addition to causing inhibition of cell proliferation, RIAM silencing led to higher susceptibility to cell apoptosis. Together, these data suggest that defective activation of these kinases in RIAM-silenced cells could account for inhibition of melanoma cell growth and that RIAM might contribute to the dissemination of melanoma cells.

Rap1 belongs to the Ras family of small GTPases, which are molecular switches that couple extracellular signals with a variety of cellular responses, such as cell proliferation and survival, cell adhesion, and cell polarity (1–3). Rap1 activation is regulated by guanine-nucleotide exchange factors, which stimulate exchange of bound GDP by GTP, and by GTPase-activating proteins, which promote GTP hydrolysis (4). The GTP-associated form of Rap1 is responsible for interaction with its effectors, which then transmit the signaling necessary to generate cell responses.

Rap1-GTP-interacting adaptor molecule (RIAM)[3] is an effector protein for Rap1 that belongs to the MRL (Mig-10/RIAM/Lamellipodin) family of adaptor proteins (5). RIAM contains an N-terminal coiled-coil region, a central Ras association, and pleckstrin homology domains, a C-terminal region rich in prolines, as well as several FPPP motifs with the potential of interacting with ENA-VASP proteins. RIAM is broadly expressed, and it was first characterized as a molecule that promotes Rap1-dependent β1 and β2 integrin activation on T lymphocytes (5). Subsequent work demonstrated that Rap1-RIAM association favors talin targeting to the plasma membrane through direct talin interaction with an N-terminal segment of RIAM, a process that contributed to integrin activation (6, 7). Furthermore, RIAM co-localizes with talin in lamellipodia (6), representing a mechanism that could help to localize activated integrins at these cell membrane protrusions. In addition, recent data indicated that an MRL ortholog in *Drosophila* called *pico* is required for tissue growth (8), therefore widening the functional potential of MRL proteins in the control of different cellular responses.

RIAM also regulates T cell receptor-mediated signaling. RIAM is recruited to immunological synapses during T cell-antigen presenting cell interactions (9). Notably, the T cell kinases ZAP-70, Fyn, and Lck can associate to RIAM and promote its tyrosine phosphorylation (10). Moreover, RIAM silencing leads to impairment in Ras-dependent signaling and

* This work was supported by Grants SAF2008-00479 from the Ministerio de Ciencia e Innovación (to J. T.), Grants SAF2007-60578 and CCG08-UCM/SAL-4259 from the Ministerio de Ciencia e Innovación (to E. M. L.), Grant RETICS RD06/0020/0011 from the Ministerio de Ciencia e Innovación (to J. T.), Grant BFU2007-66443 from the Ministerio de Ciencia e Innovación (to C. C.), a 2006 Grant from the Fundación Ramón Areces (to P. S.-M.), Grant EU-FP7-MetaFight, European Union HEALTH-2007-201862 (to J. T. and S. S.), a grant from the Swedish Cancer Society and the Swedish Research Council (to S. S.), Grant 2RO1 AI43552 (to V. A. B.), and by a grant from the Fundación de Investigación Científica de la Asociación Española Contra el Cáncer (to R. A. B.).

[S] The on-line version of this article (available at http://www.jbc.org) contains supplemental Figs. S1–S8 and Videos 1–4.

[1] Both authors contributed equally to this work.

[2] To whom correspondence should be addressed. Tel.: 34-91-8373112; Fax: 34-91-5360432; E-mail: joaquint@cib.csic.es.

[3] The abbreviations used are: RIAM, Rap1-GTP-interacting adaptor molecule; MRL, Mig-10/RIAM/Lamellipodin; CA, constitutively active; MLC, myosin light chain; PARP, poly(ADP-ribose) polymerase; SCID, severe combined immunodeficiency.

to defective translocation of phospholipase C-γ1 to the actin cytoskeleton, resulting in inhibition of T cell activation (10).

Rap1 was shown to be activated in human melanoma cell lines and metastatic melanoma tissue, and it was proposed that its activation might control melanoma cell adhesion and migration (11). Similarly, Rap1 activation correlates with high metastatic potential in prostate cancer cell lines, which was associated with a decrease in the expression of Rap1GAP (12). Examination of the cancer transcriptome profiles from the Oncomine database reveals that RIAM mRNA is found in a significant proportion of metastatic melanoma samples. Therefore, the potentially expressed RIAM protein might regulate tumor cell motility upon binding to activated Rap1. Here, we show that RIAM protein is expressed in human metastatic melanoma tissue and in melanoma cell lines, and we have used highly invasive human melanoma cell lines as models to study the role of RIAM in melanoma cell invasion. The results indicated that RIAM is required during melanoma cell invasion and that it controls melanoma cell growth and metastasis in an *in vivo* xenograft model.

EXPERIMENTAL PROCEDURES

Cells, Antibodies, and Reagents—The human melanoma cell line BLM was cultured as described previously (13). Anti-RIAM antibodies have been reported earlier (5); anti-Vav2 antibodies were from Dr. Xosé Bustelo (Centro de Investigación del Cáncer, Salamanca); control P3X63 and Lia1/2.1 integrin anti-β1 were from Dr. Francisco Sánchez-Madrid (Hospital de la Princesa, Madrid, Spain), and 15/7 anti-β1 was from Dr. Ronen Alon (Weizmann Institute of Science, Rehovot, Israel). Anti-CXCR4 was from R&D Systems (Minneapolis, MN), and Rap1, PARP, RhoA, phosphotyrosine, and Myc 9E10 antibodies were from Santa Cruz Biotechnology (Santa Cruz, CA). Anti-β-actin, anti-talin, anti-HA, and anti-His were from Sigma; anti-Erk1/2, anti-phospho-Erk1/2, anti-Akt, anti-phospho-Akt (Ser-473), anti-phosphomyosin phosphatase (Thr-696), anti-H-Ras, and anti-cleaved caspase-3 (Asp-175) were from Cell Signaling Technology (Danvers, MA); anti-procaspase-3 was from BD Biosciences, and anti-MLC antibodies were from Invitrogen. Anti-human melanoma HMB-45 was from Dako (Glostrup, Denmark). CXCL12 was purchased from R&D Systems; EGF and IGF-1 were from PeproTech (London, UK); fibronectin was from Roche Diagnostics, and collagen I and cisplatin were from Sigma.

Vectors, RNA Interference, Transfections, and PCR—HA-fused pcDNA3.1 vectors coding for wild type and constitutively active Rap1 (G12V) were from The Missouri S&T cDNA Resource Center (Rolla, MO). To obtain BLM cells stably overexpressing RIAM, its cDNA (5) was cloned into pcDNA3.1-Myc or pcDNA4MaxC-His vectors. Cells were either electroporated with pcDNA3.1-RIAM-Myc or co-transfected with pcDNA4MaxC-RIAM-His and pBabe-puro vectors using Lipofectamine (Invitrogen) or jetPrime (PolyPlus, Illkirch, France). Transfectants were selected and maintained in the presence of G418 or puromycin, respectively. Vectors coding for GFP-fused forms of wild type RhoA and Vav2 and activated V14-RhoA and Vav2 have been reported (14). To interfere with Rap1 expression we used the following siRNAs: siRap1A.1 sense strand, GAUAGAAGAUUCCUACAGAdTdT; siRap1A.2 sense strand, AUCAUGUCUGCUGCUCUAGdTdT, or a pSuper-Rap1 shRNA vector based on the Rap1A.1 siRNA sequence. siRNA for RIAM had the following sequences: siRIAM 1 sense strand, GGAAGACUCUCUAUGAUAAdTdT; siRIAM 2 sense strand, GGACAACCUUUUCGAGAAAdTdT; and siRIAM 3 sense strand, CUAUGGGACUCAGCAUAAAdTdT. Control siRNA was as described previously (14). Cells were transfected with siRNAs using X-tremeGENE (Roche Diagnostics) or with pSuper vectors using Lipofectamine, and transfectants were tested in the different assays 48 h post-transfection. To detect RIAM expression by PCR, we used the primers 5′-AAAGCGCCCACTGACTATTG-3′ and 5′-CGTTGCCTCTCTTCTTTTGC-3′ and GoTaq DNA polymerase (Promega, Madison, WI). Human GAPDH primers were as reported previously (13).

Lentiviral Gene Transfer and Animal Studies—pLL3.7 or pLL3.7-shRIAM (5) vectors were used to obtain mock or RIAM-silenced cells. Packaging was performed with HEK293T cells, and viral supernatants were used to infect target cells that were selected by cell sorting based on their GFP expression. BALB/c SCID mice (Harlan, Indianapolis, IN) maintained under specific pathogen-free conditions were employed for xenograft studies. The Cientificas Ethics Committee of the Consejo Superior de Investigaciones (Madrid, Spain) approved the protocols used for experiments with mice. Mice were injected subcutaneously in the lateral thoracic wall or intravenously into the tail vein with 1×10^6 cells. Mice were inspected daily for tumor growth and were killed when signs of respiratory stress were noted or when subcutaneous tumors reached volumes between 1.5 and 2 cm^3.

Invasion, Migration, and Adhesion Assays—Invasions across Matrigel were done as established previously (13). The lower compartments of chambers were filled with invasion medium with or without CXCL12, and invasive cells were counted under a microscope. We performed wound healing assays to study cell migration. For this, 1-mm-wide wounds were done across confluent cell monolayers on Matrigel-coated plates, and cultures were incubated with or without CXCL12. For adhesion assays, cells were labeled, as shown previously (15), and loaded in triplicate on 96-wells dishes (Costar, Cambridge, MA) coated with fibronectin (8 μg/ml) or collagen I (1–2 μg/ml). Cells were allowed to adhere, and following washing to remove unbound cells, adhesion was quantified using a fluorescence analyzer (POLARstar Galaxy; Offenburg, Germany).

Time-lapse Video Microscopy—Time-lapse analyses in migration experiments were performed using chemotaxis chambers (Ibidi, Martinsried, Germany) coated with Matrigel, using the described method (16). CXCL12 was added in the upper reservoir, and cell movement was tracked (2 min for each frame for 5 h) using a Live Cell Imaging microscope. Euclidean mean distance was assessed with ImageJ software. For protrusion dynamics, paxillin-dsRed2-transfected cells were seeded at 5000 cells/well on fibronectin-coated (10 μg/ml) glass-bottom 96-well plates. Cells were allowed to attach for 45 min, and subsequently, images were taken every 10 min using a Nikon A1R confocal microscope with a ×60 oil-immersion objective.

Three-dimensional Gel Cultures, Confocal Microscopy, and Immunohistochemistry—Rat tail collagen I (3.6 mg/ml) (Millipore, Billerica, MA) was equilibrated with $NaHCO_3$/NaOH buffer to meet neutral pH, and immediately mixed with 10× DMEM and cells to have a final mixture of 0.8 mg/ml collagen I, 2× DMEM, 2.5% FBS suspension (2×10^5 cells/ml). 20 μl drops of this mixture were allowed to polymerize at 37 °C, and resulting gels were covered with DMEM/serum and incubated for 24–72 h. Cells were stained with DAPI (0.3 μM) and imaged using a Leica TCS-SP2-AOBS-UV and Nikon A1R confocal microscope with ×63 water-immersion and ×60 oil-immersion objectives. The Ethical Committee at Hospital Universitario Gregorio Marañón approved the protocols and process involving human melanoma samples. For immunohistochemistry, melanoma metastases from lymph nodes were immediately frozen, and acetone-fixed 4-μm-thick sections were first incubated with 10% nonimmune goat serum. Samples were then incubated for 1 h at 23 °C with the appropriated antibodies or isotype-matched control antibodies. All antibodies were first tested for reactivity on lymphoid tissue and skin. The slides were mounted using an aqueous permanent mounting medium (DAKO). Confocal microscopy images were captured using a Leica SP2-AOBS confocal microscope.

Immunoprecipitation, Immunoblotting, and GTPase Assays—For immunoprecipitation, melanoma cells were lysed (17) and extracts incubated with antibodies followed by specific coupling to protein A- or G-Sepharose beads, as established previously (18). After SDS-PAGE, proteins were subjected to immunoblotting with primary antibodies, followed by incubation with horseradish peroxidase-conjugated secondary antibodies and detection with chemiluminescent substrate (Pierce). Rap1, RhoA, and H-Ras GTPase assays were performed on cells incubated in suspension with CXCL12 (13). Upon cell lysis, aliquots from extracts were kept for total lysate controls, and the remaining volume was incubated with GST-Ral-GDS (for active Rap1), GST-C21 (for active RhoA), or GST-Raf-RBD (for active H-Ras) fusion proteins in the presence of glutathione-agarose beads. Eluted proteins were subjected to immunoblotting with Rap1, RhoA, or H-Ras antibodies.

Cell Proliferation and Cytotoxicity Assays—Cell proliferation was assessed with the 3-(4,5-dimethylthiazol-2-yl)-2,5-diphenyltetrazolium bromide assay. Cells (8×10^3/well) were seeded in 96-well plates, incubated for 16 h, and subsequently stained with 0.5 mg/ml thiazolyl blue tetrazolium bromide (Sigma). Resulting formazan was resuspended with 200 μl of DMSO/well, and absorbance was read at 540 nm. Soft agar assays were performed as described previously (19). For cytotoxicity assays, cells were treated with cisplatin or H_2O_2; nonadherent cells were removed, and monolayers of surviving cells were fixed with paraformaldehyde. Upon staining with crystal violet, cells were washed and resuspended in acetic acid (33%), and absorbance was determined at 570 nm.

Statistical Analyses—Data were analyzed by one-way analysis of variance followed by Tukey-Kramer multiple comparisons. In both analyses, the minimum acceptable level of significance was $p < 0.05$.

RESULTS

Rap1 and RIAM Are Required for Invasion of Melanoma Cells—Rap1 in the highly metastatic human BLM melanoma cell line was found to be basally activated, but its activation was further increased upon exposure to CXCL12 (Fig. 1*A*), a chemokine that promotes melanoma cell invasion following binding to its receptor CXCR4 (13, 20). Rap1 silencing with two different siRNAs and with shRap1 led to defective invasion across the three-dimensional Matrigel layers in response to CXCL12 (Fig. 1, *B* and *C*). Conversely, cells transfected with constitutively active Rap1 exhibited an increase in invasion compared with Rap1 WT or mock counterparts (Fig. 1*D*). These data indicate that the chemokine-promoted melanoma cell invasion needs Rap1 function.

Earlier work demonstrated that GTP-bound active Rap1 interacts with RIAM (5). To study if RIAM was expressed in human melanoma cells, we performed immunohistochemistry on metastatic melanoma surgical specimens using anti-RIAM antibodies and antibodies to the specific melanoma marker HMB-45. The analyses revealed low to medium RIAM expression on melanoma cells from macroscopically infiltrated lymph nodes (7 of 8 cases) (Fig. 2*A*; and supplemental Fig. S1), as well as on stromal components of the tumor microenvironment. The pattern of cellular RIAM distribution and localization inside the tumors was heterogeneous. Thus, some melanoma cells displayed a predominant cytoplasmic localization of RIAM, whereas in other cells RIAM was also found on cell membrane regions. Furthermore, melanoma cells positive for RIAM expression were detected across the tumoral mass but also on the invasive borders of the tumors. In addition to its expression on metastatic melanoma tissue, RIAM was found to be expressed on the melanoma cell lines BLM, MeWo, SK-Mel-147, and SK-Mel-173, whereas its expression was undetectable in Mel57 cells (supplemental Fig. S2*A*). Pulldown assays using the GST-Ral-GDS fusion protein showed that RIAM binds to Rap1-GTP in chemokine-stimulated BLM melanoma cells (Fig. 2*B*).

To investigate if RIAM is needed for melanoma cell invasion, BLM cells were infected with lentiviral vectors designed for stable RIAM silencing (5). Two different transfectants, D11 and F7, displayed between 80 and 90% decrease in RIAM expression compared with mock transfectants (Fig. 2*C*, *top panel*; and supplemental Fig. S2*B*). Control experiments revealed no alterations in CXCR4 or β1 integrin expression levels in these transfectants (data not shown). Invasion in response to CXCL12 was blocked in D11 and F7 cells (Fig. 2*C*, *bottom panel*), as well as in an additional RIAM-depleted subline, F8-luc, engineered to express luciferase for future *in vivo* bioluminescence studies (supplemental Fig. S2*C*). Moreover, transient knockdown of RIAM by siRNA RIAM 2 and 3 led to strong inhibition of invasion toward CXCL12, whereas partial RIAM depletion by siRNA RIAM 1 resulted in a modest inhibition of invasiveness (Fig. 2*D*). To test if defective invasion shown by RIAM-silenced BLM cells could also be detected using stimuli other than CXCL12, we analyzed cell invasion toward serum. Results revealed that D11 stable transfectants as well as cells transfected with RIAM siRNA had a blockade of invasiveness in

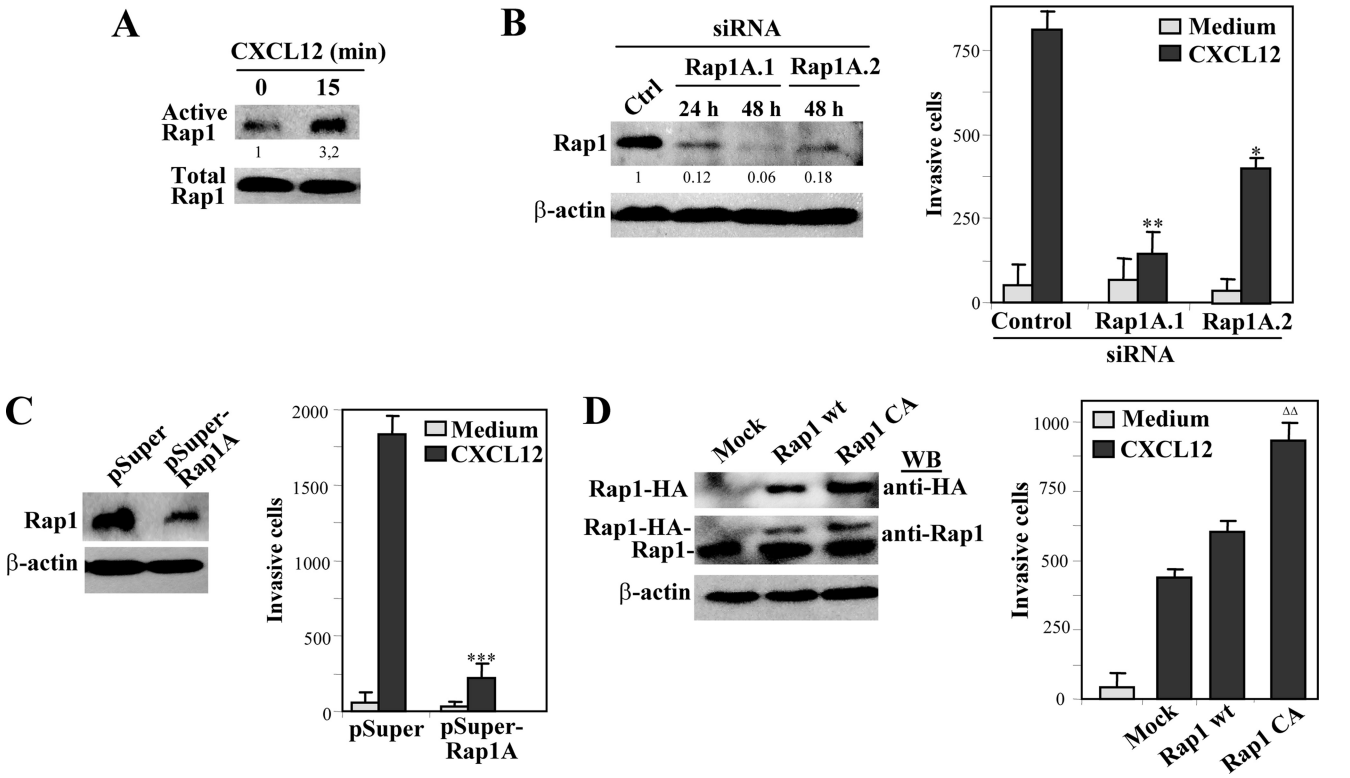

FIGURE 1. **CXCL12-promoted melanoma cell invasion is dependent on Rap1.** *A,* BLM melanoma cells were incubated with or without CXCL12 and subsequently subjected to Rap1 GTPase assays. *Numbers* below the gel represent densitometer analyses in arbitrary units. *B,* BLM cells were transfected with control (*Ctrl*) or the indicated Rap1A siRNA, and transfectants were analyzed by immunoblotting with anti-Rap1 antibodies (*left panel*) or tested in invasion assays across Matrigel in response to CXCL12 (*right panel*). *C,* cells were transfected with pSuper or pSuper-Rap1A vectors, and transfectants were analyzed by immunoblotting (*left panel*) or subjected to invasion assays (*right panel*). *D,* BLM cells were transfected with wild type Rap1 (*Rap1 wt*), constitutively active Rap1 (*Rap1 CA*), or empty vectors (*Mock*), and transfectants were analyzed by Western blotting with anti-Rap1 or anti-HA antibodies (*left panel*) or subjected to invasion assays across Matrigel (*right panel*). ***, invasion was significantly inhibited, $p < 0.001$; **, $p < 0.01$, or *, $p < 0.05$. All invasion experiments were done with duplicate samples. (*B*, $n = 4$; *C*, $n = 3$). $^{\Delta\Delta}$Invasion was up-regulated compared with invasion by mock cells, $p < 0.01$ ($n = 2$). Anti-β-actin antibodies were used to control protein loading in Western blots.

response to serum (supplemental Fig. S2*D*). Further support for the important role of RIAM in melanoma cell invasion came from experiments using BLM cells overexpressing His- or Myc-tagged RIAM, which exhibited a remarkable up-regulation of invasiveness compared with mock transfectants (Fig. 2*E*). Importantly, defective invasion of RIAM-depleted D11 cells was rescued by RIAM-His overexpression (Fig. 2*F*), indicating that deficient invasion was specifically due to RIAM knockdown. Transfection of RIAM-His in Rap1 siRNA transfectants reversed their defective invasion, whereas active Rap1 was unable to recover the impairment in invasion displayed by siRIAM transfectants (Fig. 2*G*). These results strongly suggest that RIAM acts downstream of Rap1 during chemokine-stimulated melanoma cell invasion. To analyze if RIAM silencing in another RIAM-positive, highly invasive melanoma cell line led to deficient invasion, we used MV3 cells, which displayed impaired invasiveness following RIAM depletion (supplemental Fig. S2*E*). The defect in the invasion of RIAM-silenced cells was not due to alterations in secretion or expression of MMP-2 or MT1-MMP, two metalloproteinases involved in CXCL12-promoted melanoma cell invasion (14), or of MMP-9 (supplemental Fig. S2*F*). Together, these data indicate that melanoma cell invasion requires activation of the Rap-1-RIAM signaling pathway.

Directional Persistence of Migration Is Defective in RIAM-silenced Melanoma Cells—In addition to their deficient invasion across three-dimensional Matrigel layers, wound closure assays showed that RIAM-depleted BLM cells displayed a significant inhibition of migration in the presence of CXCL12 (Fig. 3*A*). To investigate the mechanisms behind their impaired migration, we first analyzed migration by time-lapse microscopy in chemotaxis chambers. Mock cells displayed Euclidean mean distance migratory values that were more than 2-fold higher than those from RIAM knockdown transfectants, indicating that RIAM depletion affected persistent migration directionality (Fig. 3*B*; see also supplemental Videos 1 and 2). A close examination at membrane protrusions during migration revealed that although mock cells exhibited dynamic ruffle and filopodia extensions, cells depleted for RIAM showed periodic waves of lamellae protrusions that lead to a rounded morphology (Fig. 3*C*; and supplemental Videos 3 and 4).

Activation of Vav2/RhoA-dependent Signaling Is Impaired in RIAM-depleted Melanoma Cells—The deficiency in persistent migration directionality of RIAM-silenced cells might reflect a defective cell polarization, which could arise from alterations in cell contractility (21). As stress fiber formation and contractility require Rho GTPase-dependent activation of the MLC of myosin II (22, 23), we examined whether activation of RhoA and

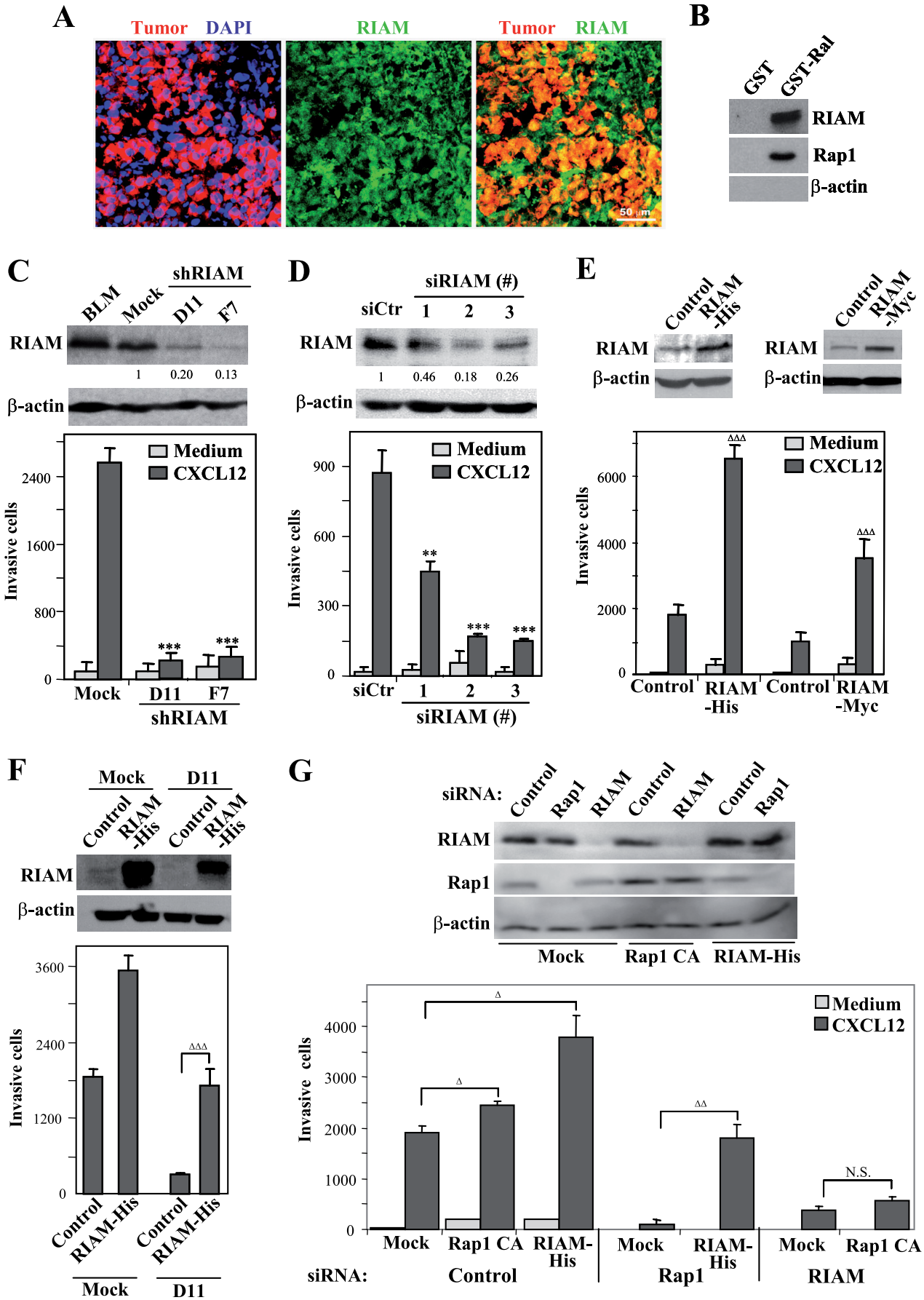
A
Tumor DAPI
RIAM
Tumor RIAM
50 μm
B
GST
GST-Ral
RIAM
Rap1
β-actin
C
shRIAM
BLM
Mock
D11
F7
RIAM
1
0.20
0.13
β-actin
Medium
CXCL12
Invasive cells
2400
1600
800
0
***
***
Mock
D11
F7
shRIAM
D
siRIAM (#)
siCtr
1
2
3
RIAM
1
0.46
0.18
0.26
β-actin
Medium
CXCL12
Invasive cells
900
600
300
0
**
***
***
siCtr
1
2
3
siRIAM (#)
E
Control
RIAM -His
Control
RIAM -Myc
RIAM
β-actin
RIAM
β-actin
Medium
CXCL12
Invasive cells
6000
4000
2000
0
ΔΔΔ
ΔΔΔ
Control
RIAM -His
Control
RIAM -Myc
F
Mock
D11
Control
RIAM -His
Control
RIAM -His
RIAM
β-actin
Invasive cells
3600
2400
1200
0
ΔΔΔ
Control
RIAM-His
Control
RIAM-His
Mock
D11
G
siRNA:
Control
Rap1
RIAM
Control
RIAM
Control
Rap1
RIAM
Rap1
β-actin
Mock
Rap1 CA
RIAM-His
Medium
CXCL12
Invasive cells
4000
3000
2000
1000
0
Δ
Δ
ΔΔ
N.S.
Mock
Rap1 CA
RIAM-His
Mock
RIAM-His
Mock
Rap1 CA
siRNA:
Control
Rap1
RIAM

MLC may be altered in RIAM-silenced cells. We first analyzed phosphorylation of Vav2, which is a guanine-nucleotide exchange factor activator molecule for RhoA (24, 25). Both Vav2 tyrosine phosphorylation and Vav2 binding to RhoA following CXCL12 stimulation were defective in D11 transfectants compared with mock counterparts (Fig. 4*A*), which were associated with impairment of RhoA activation (Fig. 4*B*). Instead, the degree of tyrosine phosphorylation of p190RhoGAP, a GTPase-activating protein for RhoA, was similar in mock and D11 cells (data not shown). RhoA activates its downstream effector ROCK, which in turn phosphorylates MLC (23). As a readout of ROCK activity, we determined the phosphorylation at Thr-696 of one of its downstream targets, the myosin phosphatase subunit (MYPT1). The results showed a deficient MYPT1 phosphorylation in response to CXCL12 in RIAM-knockdown cells (Fig. 4*C*). Once phosphorylated, myosin II assembles into myosin filaments and associates with actin filaments for generation of contractile stress fibers that are needed for cell migration (26). We found that the defect in RhoA-ROCK activation in D11 cells was associated with a decrease in MLC phosphorylation levels (Fig. 4*D*), suggesting that activation of a Vav2-RhoA-ROCK-MLC pathway is impaired in RIAM-silenced melanoma cells.

To determine whether altered Vav2-RhoA activation in RIAM knockdown cells accounted for inhibition of melanoma cell invasion, we expressed constitutively active forms of Vav2 and RhoA (Vav2 CA and RhoA CA, respectively) in mock and D11 cells, and we tested transfectants in invasion assays. Overexpression of Vav2 CA in D11 cells resulted in rescue of RhoA activation as well as to a partial recovery of invasion (Fig. 4*E*). Furthermore, overexpression of RhoA CA in D11 cells also led to a partial rescue of invasion compared with the same cells transfected with RhoA WT (Fig. 4*F*). Similarly, F8-Luc cells transfected with RhoA CA displayed higher invasion than the same cells transfected with RhoA WT forms (supplemental Fig. S3). These results indicate that impaired invasiveness shown by RIAM-silenced BLM melanoma cells involves a defect in Vav2-RhoA-ROCK-MLC activation.

Association between Talin and β1 Integrin and β1-mediated Adhesion Are Impaired in RIAM-depleted Melanoma Cells—Analyses of cell distribution of endogenous and transfected RIAM revealed that it was found at the edges of cell protrusions, usually showing a patchy distribution, as well as diffusely in the cytoplasm of BLM cells (supplemental Fig. S4*A*). Furthermore, RIAM-His co-precipitated with talin in these cells (supplemental Fig. S4*B*), in agreement with RIAM-talin association previously reported in other cell types (7). Notably, RIAM silencing led to defective association of talin with the integrin β1 subunit (Fig. 5*A*). As also shown before (27), talin co-precipitation with anti-β1 antibodies was specific, as it was not detected in talin siRNA transfectants, and these antibodies co-precipitated the counterpart α4 integrin subunit but not PARP (supplemental Fig. S5). Moreover, RIAM-His expression in RIAM-depleted D11 cells led to recovery of talin β1 association (Fig. 5*B*), indicating that the assembly between these proteins requires RIAM. Linked to defective talin β1 association in RIAM-knockdown cells, they displayed a decrease in β1 integrin-dependent attachment to fibronectin and type I collagen compared with control transfectants (Fig. 5, *C* and *D*, *left panels*). On the contrary, RIAM overexpression resulted in up-regulated cell adhesion to fibronectin (Fig. 5*C*, *right panel*). As β3 integrin expression is negligible in BLM melanoma cells (data not shown), together with the blockade of cell attachment by anti-β1 mAb, our adhesion results clearly reflect the activity of β1 integrins.

Given that talin β1 association is an event that correlates with integrin activation (28) and that this association is impaired in RIAM-silenced cells, we tested the binding of 15/7, an anti-β1 antibody that detects high affinity β1 integrin conformations (29), as an indication of the degree of integrin activation in these cells. Binding of 15/7 mAb was moderately reduced in D11 transfectants compared with mock counterparts (supplemental Fig. S6*A*). Flow cytometry control experiments showed that mock and D11 cells retained similar degrees of 15/7 mAb binding upon exposure to Mn^{2+}, a positive activator of integrin affinity. To study if reduced 15/7 mAb binding to RIAM-depleted cells could reflect possible changes in integrin ligand binding, we used biotin-labeled fibronectin in soluble binding experiments. The results showed minimal and nonstatistically significant differences in fibronectin binding between mock and D11 cells (supplemental Fig. S6*B*). In addition, confocal microscopy together with software-assisted custom-patch morphology analyses showed that there were no gross alterations in the degree of β1 integrin clustering in D11 cells compared with mock counterparts (supplemental Fig. S6*C*). These results suggest that no differences in β1 integrin avidity for their ligands exist between both cells. Together, these data indicate that RIAM depletion affects talin β1 association, which leads to alterations in β1 affinity conformations but with minimal effects on ligand binding.

RIAM-silenced Melanoma Cells Have Decreased Erk1/2 and Akt Activation—As also reported in T cells (10), knockdown of RIAM in melanoma cells led to inhibition of Ras activation, and

FIGURE 2. **RIAM is required for melanoma cell invasion.** *A,* immunohistochemical analysis of RIAM expression on melanoma lymph node metastasis. Sections were stained with the melanoma-specific marker HMB-45 (tumor) or with anti-RIAM antibodies or with DAPI to visualize nuclei. Sample 82 is shown. Additional analyses of melanoma specimens are shown in supplemental Fig. S1. *B,* lysates from BLM cells exposed for 15 min to CXCL12 were incubated with GST or GST-Ral-GDS, and bound Rap1 and RIAM were detected by immunoblotting. *C,* expression of RIAM in untransfected BLM cells, and in Mock and stable RIAM knockdown transfectants (D11 and F7), was analyzed by immunoblotting with anti-RIAM antibodies (*top panel*). *Numbers* below the gel represent densitometer analyses in arbitrary units. *Bottom panel,* transfectants were tested in invasion assays across Matrigel. *D,* BLM cells were transfected with control or with the indicated RIAM siRNA, and transfectants were analyzed by immunoblotting (*top panel*) or subjected to invasion assays (*bottom panel*). *E,* BLM cells were transfected with His- or Myc-tagged RIAM vectors, and transfectants were analyzed by immunoblotting to determine RIAM-His or RIAM-myc expression (*left panel*) or subjected to invasion assays (*right panel*). *F,* mock and D11 cells were transfected with control or RIAM-His vectors, and their invasion to CXCL12 was compared with that of mock cells. *G,* BLM cells were transfected with the indicated siRNA together with Rap1 CA, RIAM-His, or mock vectors. Transfectants were analyzed by immunoblotting (*top panel*) or tested in invasion assays (*bottom panel*). (*C*, $n = 5$; *D*, $n = 3$; *E*, $n = 3$; *F*, $n = 2$; *G*, $n = 2$.) ***, invasion was significantly inhibited, $p < 0.001$; **, $p < 0.01$; $^{\Delta\Delta\Delta}$, invasion was up-regulated compared with invasion by mock transfectants, $p < 0.001$; $^{\Delta\Delta}$, $p < 0.01$; $^{\Delta}$, $p < 0.05$. Anti-β-actin antibodies were used to control protein loading in Western blots.

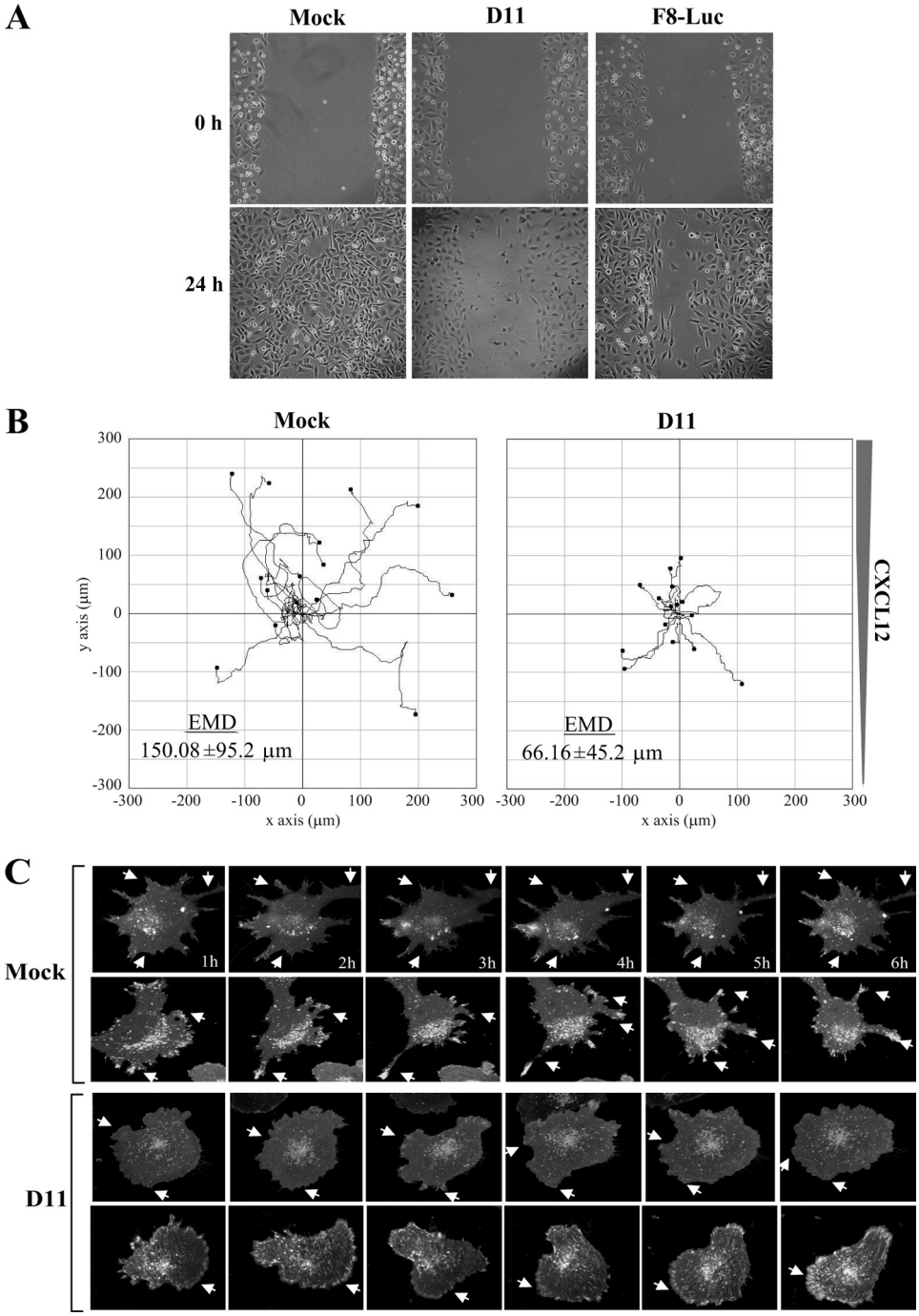

FIGURE 3. **Directional persistence of migration is deficient in RIAM-silenced melanoma cells.** *A,* transfectants in culture were tested in wound healing assays in the presence of CXCL12 (50 ng/ml). A representative result from three experiments is shown. *B,* transfectants were subjected to time-lapse microscopy experiments on Matrigel. CXCL12 (150 ng/ml) was added on the top reservoir of chambers, and migration of individual cells ($n = 15$) was tracked and represented in micrometers (*x* and *y* axis) using a common starting point in the *middle* of the graph. Shown is a representative result of three independent experiments. *EMD,* Euclidean mean distance. *C,* cells were transfected with DsRed-paxillin, and membrane protrusions were analyzed for the indicated times by time-lapse microscopy. Shown are two representative individual cells from each mock and D11 transfectant.

exposure to CXCL12 could not recover the activation to the levels shown by mock cells (Fig. 6*A*). These results suggested that Ras downstream signaling could be affected due to RIAM silencing. Indeed, activation of both Erk1/2 MAPK and the phosphatidylinositol 3-kinase (PI3K) downstream effector Akt following β1 integrin-dependent adhesion to fibronectin and type I collagen was lower in RIAM-depleted BLM melanoma transfectants than in mock counterparts (Fig. 6, *B* and *C*). Notably, Erk1/2 MAPK activation in RIAM knockdown cells was rescued following transfection of RIAM-His (Fig. 6*D*). These results indicate that RIAM silencing in melanoma cells affects activation of β1 integrin-mediated outside-in molecular signaling that regulates cell growth and survival, such as Erk1/2 MAPK and PI3K activation.

Growth factor receptors cooperate with integrins to stimulate and/or sustain the activation of MEK-Erk1/2 and PI3K-Akt

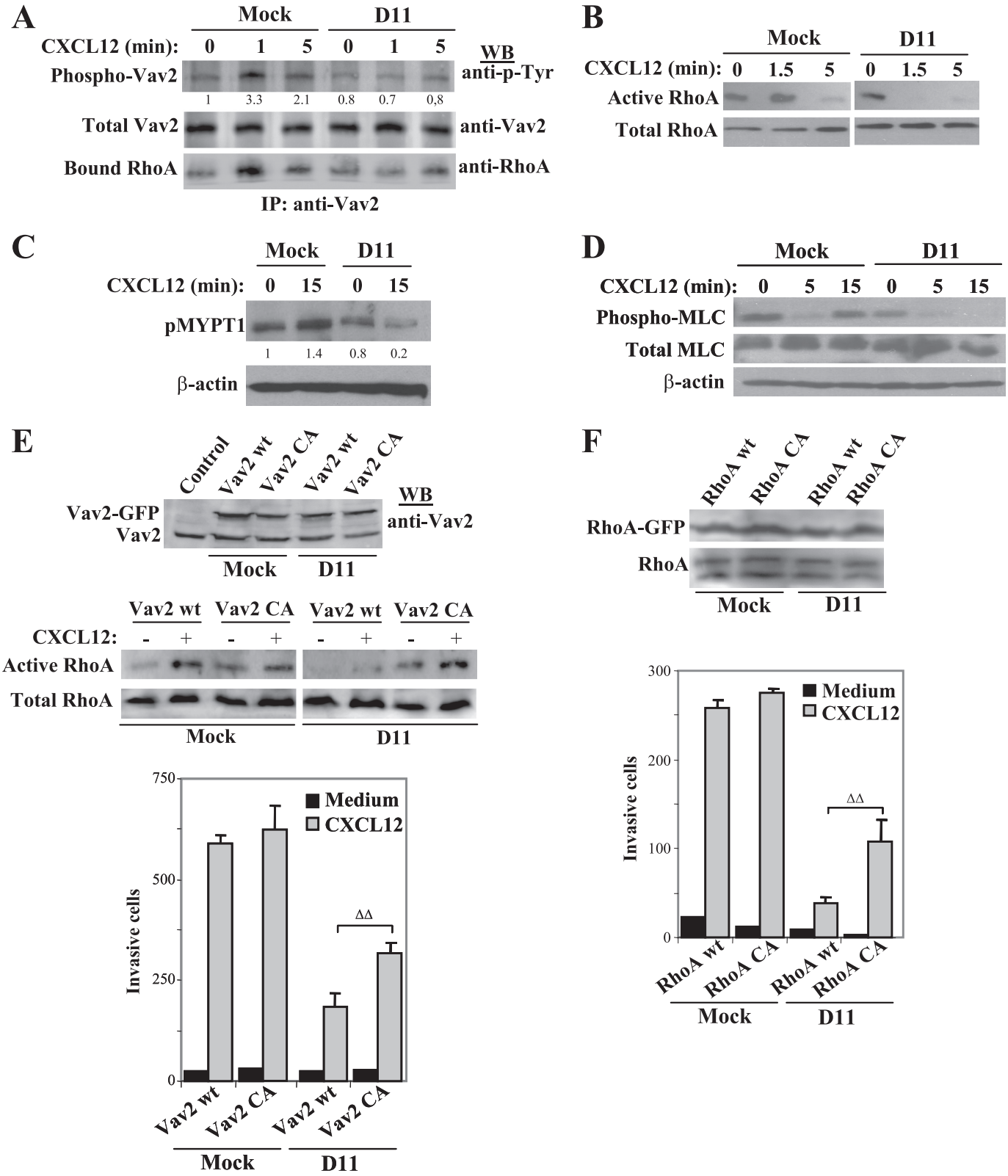

FIGURE 4. **Impaired invasion of RIAM-silenced melanoma cells involves defective Vav2-RhoA-ROCK-MLC activation.** *A,* mock or D11 cells were incubated for the indicated times with CXCL12 and subjected to immunoprecipitation (*IP*) with anti-Vav2 antibodies, followed by immunoblotting with the indicated antibodies. *Numbers* below the gel represent densitometer analyses in arbitrary units showing Vav2 tyrosine phosphorylation levels. *B–D,* cells were tested for GTPase assays to detect active RhoA (*B*) or analyzed by Western blotting for phospho-MYPT1 (*C*) or for phospho-MLC or total MLC expression (*D*). *E,* mock and D11 cells were transfected with GFP-fused wild type (*wt*) or constitutively active (*CA*) forms of Vav2, and transfectants were analyzed by immunoblotting with anti-Vav2 antibodies (*top panel*) or subjected to RhoA GTPase and invasion assays (*middle* and *bottom panels*, respectively). *F,* mock and D11 cells were transfected with GFP-fused wild type (*wt*) or constitutively active (*CA*) forms of RhoA, and transfectants were analyzed by immunoblotting with anti-RhoA antibodies (*left panel*) or tested in invasion assays (*right panel*). $^{\Delta\Delta}$, invasions of D11-Vav2 CA or D11-Rho CA transfectants were significantly higher than D11-Vav2 WT or D11-Rho WT cells, respectively, $p < 0.01$.

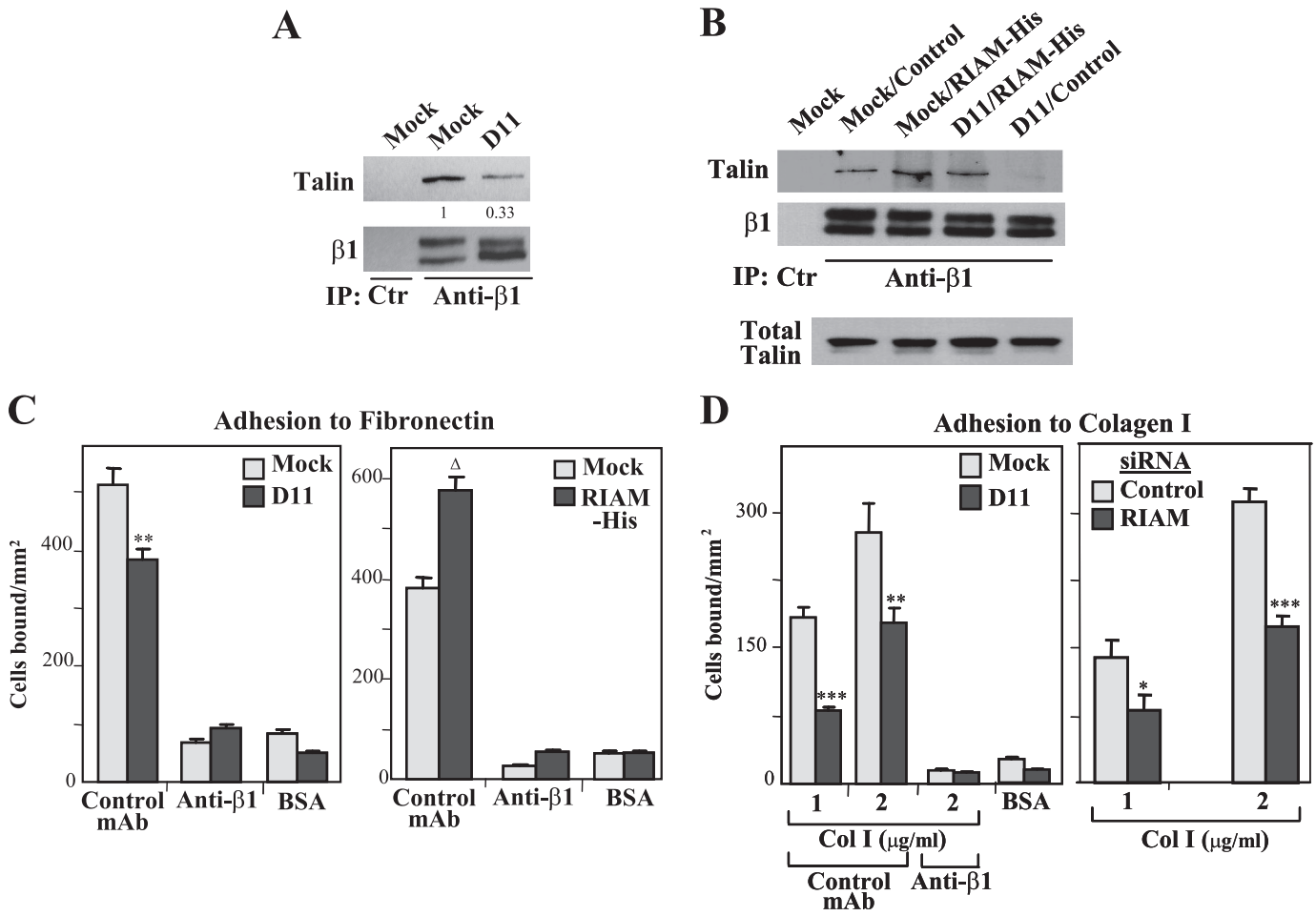

FIGURE 5. **RIAM-silenced melanoma cells have reduced talin β1 integrin association and defective β1 integrin-mediated adhesion.** *A,* transfectants were subjected to immunoprecipitation (*IP*) with control (*Ctr*) or Lia 1/2.1 anti-β1 antibodies, followed by immunoblotting with anti-talin or anti-β1 antibodies. *B,* mock or D11 cells were transfected with control or RIAM-His vectors and subjected to immunoprecipitation and Western blotting as in *A*. Total talin loading is also shown. *C* and *D,* transfectants were tested in adhesion assays (10 min, 37 °C) to fibronectin or type I collagen, in the presence of control or Lia 1/2.1 anti-β1 mAb. Basal adhesion to BSA is also displayed. ***, adhesion was significantly inhibited, $p < 0.001$; **, $p < 0.01$; or *, $p < 0.05$; or stimulated $^{\Delta}$, $p < 0.05$ ($n = 4$).

pathways (30). We therefore tested if the decreased activation of these signaling pathways in RIAM-silenced melanoma cells could be recovered by exposure to growth factors. Following incubation with EGF, starved D11 cells displayed Erk1/2 and Akt phosphorylation levels similar to those found in mock cells (Fig. 6*E*, *left panel*). When cells were exposed to IGF-1, Akt phosphorylation was comparable between mock and RIAM-depleted cells, although Erk1/2 activation was only partially recovered (Fig. 6*E*, *right panel*). These results strongly suggest that Erk1/2 and PI3K-Akt activation through RIAM is integrin-dependent and growth factor-independent.

Growth and Metastatic Properties of RIAM Knockdown Melanoma Cells—RIAM-silenced and mock melanoma cells were inoculated into SCID mice to follow their growth and dissemination. Between days 25 and 75 after subcutaneous inoculation with mock cells, all mice ($n = 13$) displayed tumor volumes between 1.5 and 2.0 cm^3, whereas only 3 of 10 or 1 of 10 mice inoculated with D11 or F7 cells, respectively, showed these tumor volumes (Fig. 7*A*). No subcutaneous tumor growth was detected in 60 and 90% of mice inoculated with D11 and F7, respectively, up to day 125.

Three weeks after intravenous inoculation with mock melanoma transfectants, mice rapidly developed lung metastases, and after 6 weeks there were no surviving mock animals (Fig. 7*B*). D11 and F7 mice had a significantly longer disease-free period (5.5–8 weeks), which was linked to a prolonged survival (Fig. 7*B*). Melanoma cells derived from lung metastases retained GFP expression and displayed invasiveness to Matrigel comparable with their original transfectants (supplemental Fig. S7, *A* and *B*), indicating that they retained their invasive properties during dissemination. Inhibition of *in vivo* tumor growth shown by RIAM knockdown melanoma cells correlated with abolishment in their capacity to form colonies in soft agar cultures compared with mock cells (Fig. 7*C*). Furthermore, D11 and F7 cells displayed a reduction in cell proliferation, and conversely, cells overexpressing RIAM-His had higher proliferation rates than mock transfectants (Fig. 7*D*). Together, these data indicate that RIAM expression contributes to *in vitro* BLM melanoma cell proliferation and confers growth and metastatic advantages to these melanoma cells in a xenograft model.

As inhibition of *in vivo* growth shown by RIAM-depleted melanoma cells might also reflect apoptosis responses, we first analyzed whether they have increased sensitivity to apoptosis-inducing agents. As a model for induction of cell apoptosis, we used cisplatin, a pro-apoptotic DNA-alkylating agent used in

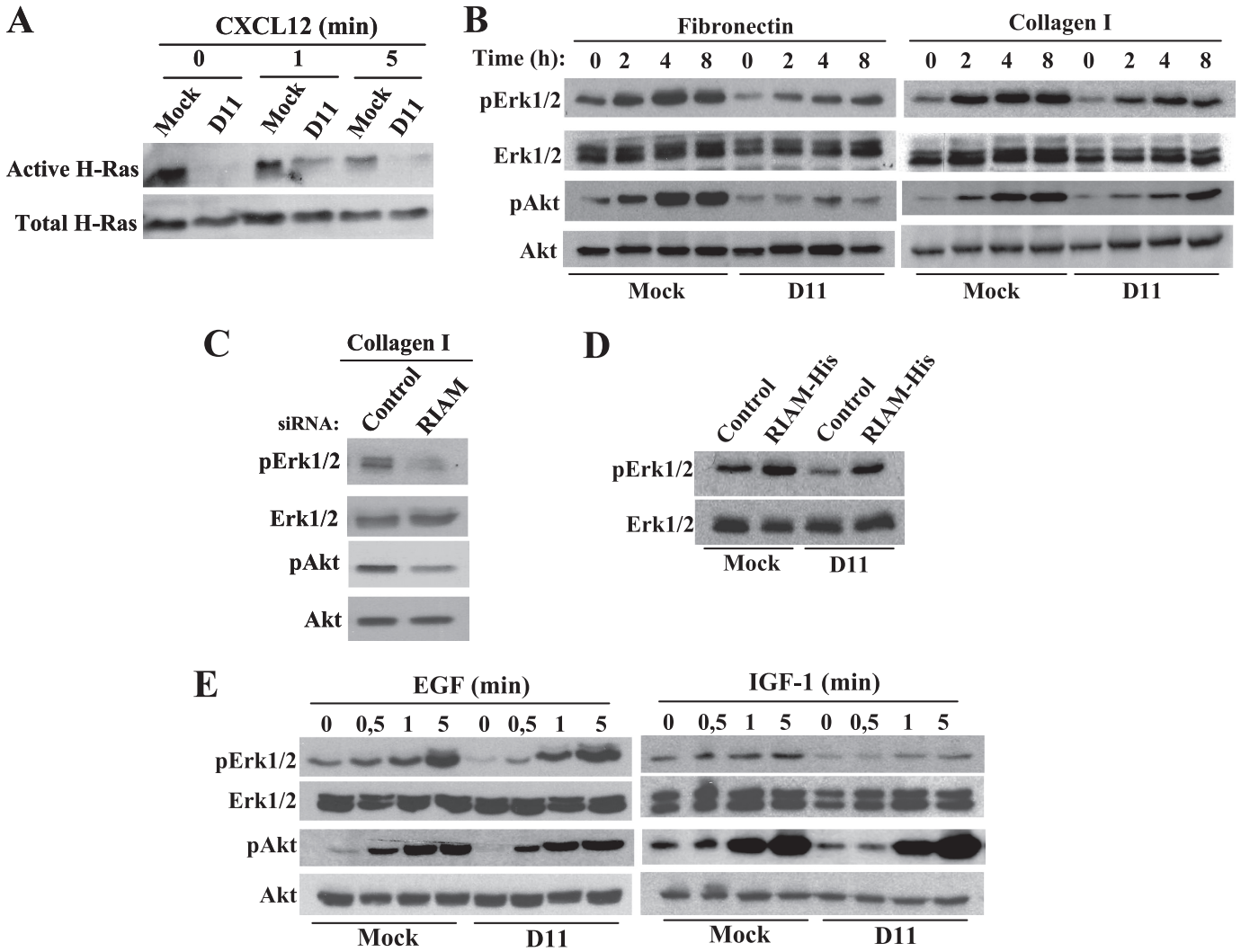

FIGURE 6. **RIAM-silenced melanoma cells have defective Erk1/2 and Akt activation.** *A,* cells were incubated for the indicated times with CXCL12 and subsequently subjected to Ras GTPase assays. *B* and *C,* transfectants were plated for the indicated times on fibronectin or collagen I, and following cell lysis, extracts were subjected to Western blotting with antibodies to phospho-Erk1/2, Erk1/2, phospho-Akt, or Akt. *D,* mock and D11 cells were transfected with control or RIAM-His vectors and subsequently analyzed by immunoblotting with phospho-Erk1/2 and Erk1/2 antibodies. *E,* transfectants were starved for 8 h and subsequently incubated for the indicated times with EGF (10 ng/ml) or IGF-1 (100 ng/ml). Cells were then lysed and subjected to immunoblotting using anti-Erk1/2 or anti-Akt antibodies.

the treatment of solid tumors (31). Cisplatin induced a dose-dependent decrease in cell survival that was of significantly higher extent in D11 and F7 than in mock cells (Fig. 8*A*, *left panel*). This observation was associated with reduced levels of procaspase-3 and with higher PARP cleavage in D11 transfectants (Fig. 8*A*, *right panel*). In addition, D11 and F7 transfectants were more susceptible than mock cells to apoptosis by the hydroxyl radicals generated from excess H_2O_2 (Fig. 8*B*). Given that melanoma cells invade across type I collagen-rich dermal connective tissue layers, we embedded mock and D11 cells in three-dimensional collagen I gels and performed caspase-3 staining and analyses of nuclei integrity as an indication of cell apoptosis. Staining of D11 cells with an antibody to cleaved caspase-3 was substantially stronger than in mock cells (Fig. 8*C*). Following 72 h in the collagen gels, RIAM-silenced cells displayed a higher proportion of compact/broken nuclei than mock cells (70 and 15%, respectively), as well as increased Hoechst staining (supplemental Fig. 8). These data indicate that cells depleted for RIAM have increased susceptibility to apoptosis.

Finally, as p38 MAPK activation is linked to cell stress and plays key roles in the control of cell proliferation and survival (32), we assessed its phosphorylation levels in mock and RIAM knockdown cells. The results showed that p38 MAPK was phosphorylated to higher levels in D11 than in mock cells when they were exposed to cisplatin (Fig. 8*D*).

DISCUSSION

We have used highly invasive human melanoma cell lines to demonstrate that their invasion requires Rap1 and its binding partner RIAM. We found that RIAM is expressed in melanoma cells in human metastatic tissue, although its expression was not restricted to melanoma cells, as other cells within the tumor microenvironment also expressed RIAM. It is not known at present whether RIAM expression on melanoma cells contributes to tissue invasion, or if its expression could be used as a prognostic value, a hypothesis that will be next studied. Notably, RIAM silencing in melanoma cells led to inhibition of

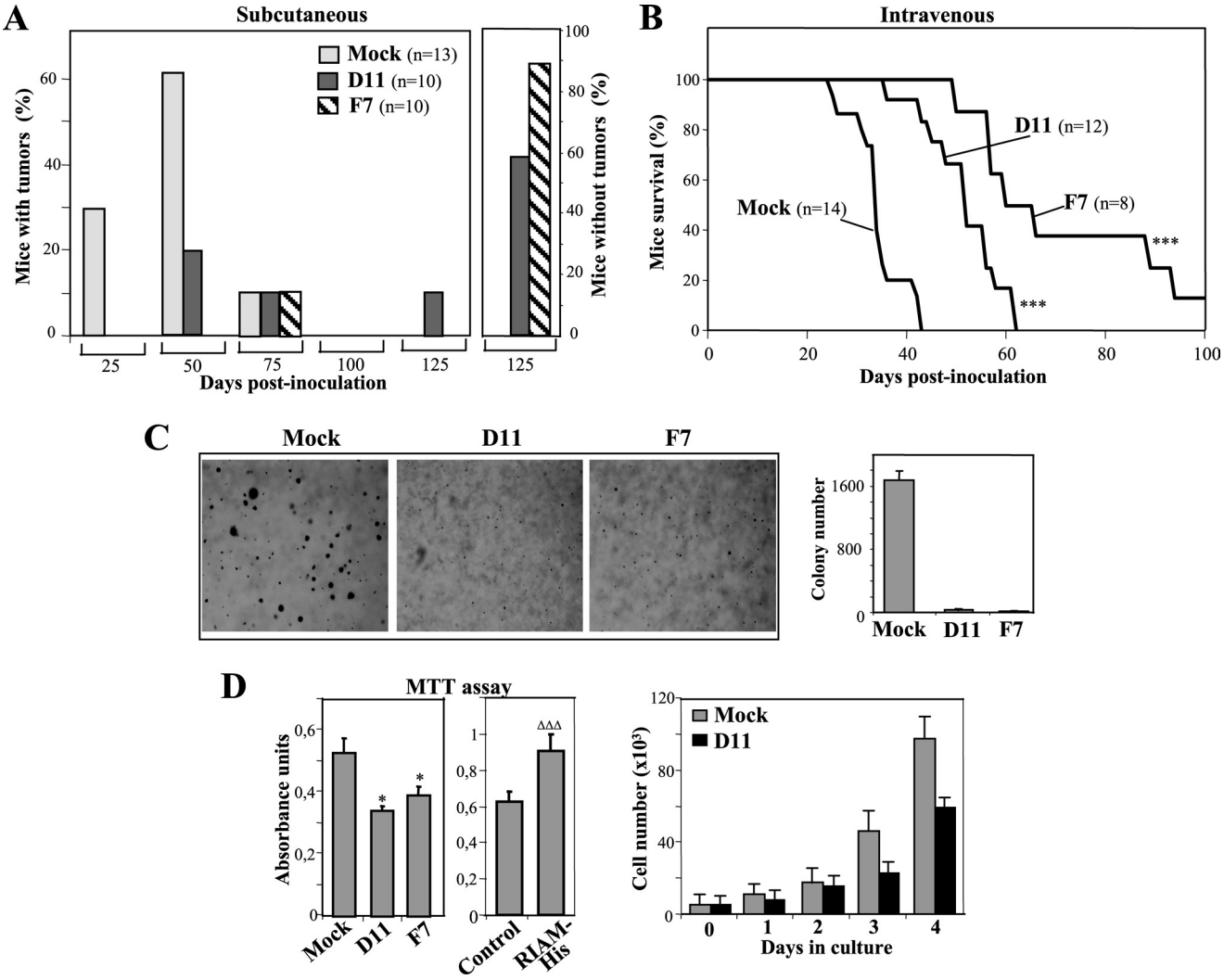

FIGURE 7. **RIAM silencing in melanoma leads to inhibition of tumor growth and delayed metastasis.** *A,* SCID mice were subcutaneously inoculated with the indicated melanoma BLM transfectants. Data show the correlation between days post-inoculation and percentage of mice with tumors (*left panel*) or tumor-free mice (*right panel*). *B,* shown are survival curves of SCID mice intravenously inoculated with the indicated melanoma transfectants (***, survival was significantly higher than mice inoculated with mock transfectants, $p < 0.001$). *C,* displayed are representative fields of anchorage-independent colony formation on soft agar (*left panel*), and quantification in mean colony numbers (*right panel, n* = 3; duplicates). Only colonies larger than 50 μm were counted. *D,* cell proliferation was determined using the 3-(4,5-dimethylthiazol-2-yl)-2,5-diphenyltetrazolium bromide (*MTT*) assay (*left panel*). *, proliferation was inhibited, $p < 0.05$, or augmented; $^{\Delta\Delta\Delta}$, $p < 0.001$ ($n = 4$). *Right panel,* cells (5×10^3) were cultured in complete medium for the indicated times and counted in Newbauer chambers ($n = 3$).

tumor growth and delayed metastasis in a SCID xenograft model, suggesting that RIAM expression on melanoma cells might indeed contribute to tumor progression.

Experiments to rescue the invasion of Rap1 and RIAM siRNA transfectants indicated that RIAM acts downstream of Rap1 for efficient cell invasion triggered by CXCL12. Defective invasion of RIAM-silenced melanoma cells arose from impairment in sustained cell migration directionality, which was associated with inhibition in the activation of a Vav2-RhoA-ROCK-MLC pathway. Furthermore, our results indicate that RIAM depletion reduces β1-dependent melanoma cell adhesion, which correlates with decreased activation of both Erk1/2 MAPK and PI3K, two central molecules that control cell growth and cell survival. In addition, to inhibit cell proliferation, RIAM silencing led to higher susceptibility to cell apoptosis.

BLM melanoma cell knockdown for RIAM displayed a predominant rounded morphology linked to impairment in the acquisition of a polarized phenotype. Myosin II-based contractility generates the force needed for cell migration, and it contributes to cell polarity and to persistent cell migration (21, 26, 33). In support for defective polarization in cells knocked down for RIAM that display impaired migration is the finding that they have deficient activation of the regulatory MLC component of myosin II. The defect in MLC phosphorylation correlated with inhibition in the activation of the Vav2-RhoA-ROCK pathway, suggesting that altered stimulation of this pathway accounts for impairment of MLC activation in these cells. Importantly, expression of constitutively active Vav2 and RhoA forms partially rescued invasion of RIAM-depleted melanoma cells, indicating that Vav2 and RhoA mediate RIAM functions. Therefore, the data suggest that inhibition of invasion in RIAM-silenced cells involves altered contractility and cell polarization due to deficient activation of a Vav2-RhoA-ROCK-MLC pathway. The structural and functional connec-

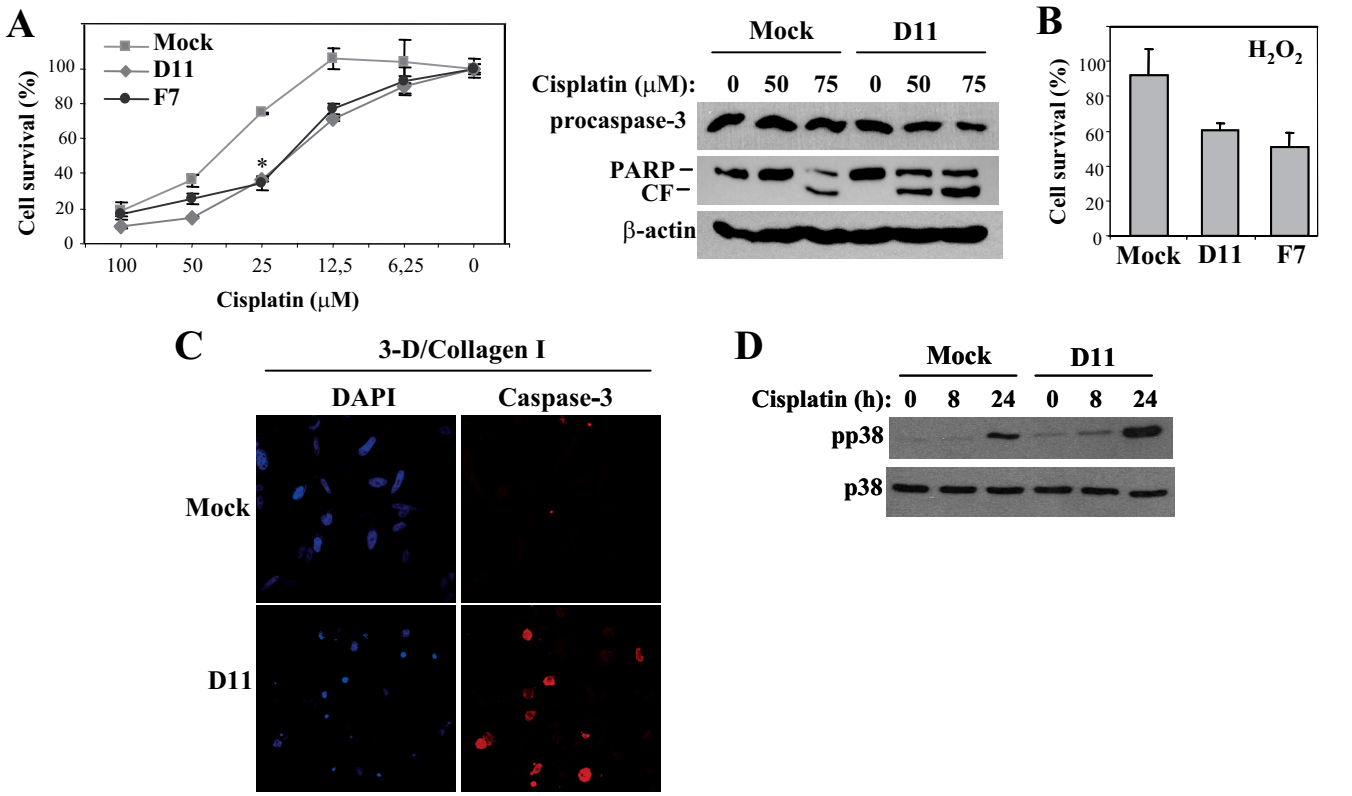

FIGURE 8. **RIAM-silenced melanoma cells have increased susceptibility to apoptosis.** *A,* melanoma transfectants were incubated for 24 h in the presence of the indicated concentrations of cisplatin, and cell survival was measured as indicated under "Experimental Procedures" (*left panel*) or cell extracts subjected to immunoblotting using antibodies to the indicated proteins (*right panel*). The PARP antibody recognizes both the intact and cleaved fragment (*CF*). *B,* cells were treated for 14 h with 3 μM H_2O_2, and cell survival was measured as above. *C,* mock and D11 cells were embedded in three-dimensional (*3-D*) type I collagen gels, stained with DAPI or with an antibody to cleaved caspase-3, and analyzed by confocal microscopy. *D,* cells were exposed for the indicated times to cisplatin (50 μM) and subsequently subjected to Western blotting for detection of phosphorylated (*pp38*) or total p38 MAPK.

tions of RIAM with this pathway are not known at present and should be the subject of future studies. A possible explanation is based on the fact that active Rap1 contributes to cell localization of Vav2 (34). Therefore, it is tempting to speculate that a Rap1-GTP/RIAM complex might recruit Vav2 to the cell membrane for subsequent Vav2 activation.

Recent work has reported that RIAM binds talin, which facilitates the recruitment of talin to β3 integrin sites and subsequent activation of these integrins (6, 7, 35). We found that, in addition to binding to Rap1, RIAM also associates with talin in melanoma cells. Interestingly, RIAM depletion led to a decrease in talin β1 integrin association that was linked to a reduction in β1 integrin-dependent cell adhesion to fibronectin and collagen I. The basis for this reduced adhesion is not known at present, but it does not seem to involve gross differences in β1 clustering or β1 integrin activation between mock and RIAM-silenced cells. A small but consistent decrease in the generation of high affinity β1 conformations in RIAM-silenced cells was detected with the 15/7 anti-β1 mAb. This is an observation that might reflect the decrease in talin β1 association in these cells, given that talin is a main protein controlling integrin activation (28). As mentioned above, RIAM-knockdown cells display a more rounded phenotype than mock cells, conceivably because of changes in the reorganization of the actin cytoskeleton, which might affect adhesion strengthening, ultimately leading to reduced cell adhesion. Therefore, our results suggest that as a result of its talin-binding capacity, RIAM possibly regulates the assembly of β1-dependent adhesive platforms that are required for efficient cell adhesion.

The reduction in β1-dependent adhesion of RIAM knockdown cells is most likely the basis for the decreased activation of Erk1/2 and the PI3K downstream effector Akt, which are well known downstream targets in outside-in signaling from integrins, involving at least cyclin D1 (30, 36). Ras represents an upstream candidate mediating integrin-dependent Erk1/2 MAPK activation that is regulated by RIAM activity. Thus, it has been demonstrated that RIAM depletion in T cells results in failure of Ras-dependent Erk1/2 activation in response to TCR stimulation (10). Indeed, we found that RIAM-knockdown melanoma cells have defective Ras activation, strongly suggesting that this defect represents a mechanism responsible for the deficient Erk1/2 activation.

One of the possible mechanisms behind the defective growth shown by RIAM-knockdown melanoma cells subcutaneously inoculated into SCID mice could be based on deficient stimulation of β1 integrin-dependent outside-in signaling pathways such as those controlled by Erk1/2 and PI3K, which are needed for cell proliferation. The levels of Erk1/2 and Akt phosphorylation detected in RIAM-depleted melanoma cells following incubation with EGF or IGF indicate that Erk1/2 and PI3K-Akt activation involving RIAM is integrin-dependent but growth factor-independent, and again it reflects the important role of upstream RIAM in the control of β1 integrin-mediated outside-in signaling. Our data suggest that when melanoma cells are in tissue culture conditions, the reduced adhesion shown by RIAM-depleted cells is

likely sufficient to result in decreased Erk1/2 and Akt activation, and only when large amounts of growth factors are exogenously provided is activation rescued. In *in vivo* conditions, limited growth factor supply and poor adhesion might lead to the observed inhibition of growth of RIAM-silenced cells.

Concomitant with the inhibition of proliferation shown by RIAM-silenced melanoma cells, they also displayed an increase in susceptibility to apoptosis than their mock counterparts. Their higher apoptosis responses were detected in two-dimensional cultured RIAM-depleted cells exposed to cisplatin, as well as when they were embedded in three-dimensional type I collagen gels, a condition that mimics connective tissue environments that must be crossed during invasion of melanoma cells. These responses might be a consequence of their defective proliferation dependent on outside-in signaling from β1 integrins. Although the αvβ3 integrin has been shown to be involved in melanoma cell survival (37, 38), it is unlikely that it plays a role in BLM cell survival, given that these cells express only background levels of this integrin (data not shown). Therefore, a decrease in proliferation and higher sensitivity to apoptosis of RIAM-depleted melanoma cells might contribute to inhibition of tumor growth of subcutaneously injected cells.

When RIAM-silenced melanoma cells were intravenously inoculated, we detected significantly longer survival of SCID mice, associated with delayed latency of lung dissemination, than in those mice injected with mock cells. Based on the impaired cell invasiveness displayed by RIAM knockdown cells, a delay in the latency could reflect a defective lung homing and invasion capacity of these cells that could retard the initial steps of lung colonization. Alternatively, melanoma cell arrival to lungs might be only modestly affected by RIAM depletion, and the extended survival of mice might reflect the reduction of melanoma cell growth because of RIAM silencing. A more permissive lung environment compared with that of primary skin tumor could later favor the growth of RIAM-depleted melanoma cells involving lung growth factors. Altogether, these results indicate that RIAM contributes to cell growth and metastasis of BLM melanoma cells. Importantly, the *Drosophila* MRL protein ortholog *pico* is required for tissue growth, and its silencing leads to reduced cell division rates (8), thus stressing the important role of MRL proteins in cell proliferation.

Acknowledgments—We thank Drs. Angeles García-Pardo, Marisol Soengas, Johannes L. Bos, José María Rojas, Rick Horwitz, Patricio Aller, and David García-Bernal for reagents and helpful discussions. Dr. Rafael Samaniego (Unidad de Microscopía Confocal, Hospital General Universitario Gregorio Marañón) and María Teresa Seisdedos are acknowledged for confocal microscopy, Dr. Pedro Lastres for cell sorting, and Manuel Moreno-Calle and Cristina Pintos-Maestro for assistance in the Animal Facility. Part of the imaging was performed at the Live Cell Imaging facility, Department of Biosciences and Nutrition at Karolinska Institutet, supported by grants from the Knut and Alice Wallenberg foundation, the Swedish Research Council, and the Center for Biosciences.

REFERENCES

1. Bos, J. L. (2005) *Curr. Opin. Cell Biol.* **17,** 123–128
2. Raaijmakers, J. H., and Bos, J. L. (2009) *J. Biol. Chem.* **284,** 10995–10999
3. Boettner, B., and Van Aelst, L. (2009) *Curr. Opin. Cell Biol.* **21,** 684–693
4. Bos, J. L., Rehmann, H., and Wittinghofer, A. (2007) *Cell* **129,** 865–877
5. Lafuente, E. M., van Puijenbroek, A. A., Krause, M., Carman, C. V., Freeman, G. J., Berezovskaya, A., Constantine, E., Springer, T. A., Gertler, F. B., and Boussiotis, V. A. (2004) *Dev. Cell* **7,** 585–595
6. Watanabe, N., Bodin, L., Pandey, M., Krause, M., Coughlin, S., Boussiotis, V. A., Ginsberg, M. H., and Shattil, S. J. (2008) *J. Cell Biol.* **181,** 1211–1222
7. Lee, H. S., Lim, C. J., Puzon-McLaughlin, W., Shattil, S. J., and Ginsberg, M. H. (2009) *J. Biol. Chem.* **284,** 5119–5127
8. Lyulcheva, E., Taylor, E., Michael, M., Vehlow, A., Tan, S., Fletcher, A., Krause, M., and Bennett, D. (2008) *Dev. Cell* **15,** 680–690
9. Ménasché, G., Kliche, S., Chen, E. J., Stradal, T. E., Schraven, B., and Koretzky, G. (2007) *Mol. Cell. Biol.* **27,** 4070–4081
10. Patsoukis, N., Lafuente, E. M., Meraner, P., Kim, J., Dombkowski, D., Li, L., and Boussiotis, V. A. (2009) *Sci. Signal.* **2,** ra79
11. Gao, L., Feng, Y., Bowers, R., Becker-Hapak, M., Gardner, J., Council, L., Linette, G., Zhao, H., and Cornelius, L. A. (2006) *Cancer Res.* **66,** 7880–7888
12. Bailey, C. L., Kelly, P., and Casey, P. J. (2009) *Cancer Res.* **69,** 4962–4968
13. Bartolomé, R. A., Gálvez, B. G., Longo, N., Baleux, F., Van Muijen, G. N., Sánchez-Mateos, P., Arroyo, A. G., and Teixidó, J. (2004) *Cancer Res.* **64,** 2534–2543
14. Bartolomé, R. A., Molina-Ortiz, I., Samaniego, R., Sánchez-Mateos, P., Bustelo, X. R., and Teixidó, J. (2006) *Cancer Res.* **66,** 248–258
15. Bartolomé, R. A., Ferreiro, S., Miquilena-Colina, M. E., Martínez-Prats, L., Soto-Montenegro, M. L., García-Bernal, D., Vaquero, J. J., Agami, R., Delgado, R., Desco, M., Sánchez-Mateos, P., and Teixidó, J. (2009) *Am. J. Pathol.* **174,** 602–612
16. Molina-Ortiz, I., Bartolomé, R. A., Hernández-Varas, P., Colo, G. P., and Teixidó, J. (2009) *J. Biol. Chem.* **284,** 15147–15157
17. Ticchioni, M., Charvet, C., Noraz, N., Lamy, L., Steinberg, M., Bernard, A., and Deckert, M. (2002) *Blood* **99,** 3111–3118
18. Bartolomé, R. A., Wright, N., Molina-Ortiz, I., Sánchez-Luque, F. J., and Teixidó, J. (2008) *Cancer Res.* **68,** 8221–8230
19. Cifone, M. A., and Fidler, I. J. (1980) *Proc. Natl. Acad. Sci. U.S.A.* **77,** 1039–1043
20. Robledo, M. M., Bartolome, R. A., Longo, N., Rodríguez-Frade, J. M., Mellado, M., Longo, I., van Muijen, G. N., Sánchez-Mateos, P., and Teixidó, J. (2001) *J. Biol. Chem.* **276,** 45098–45105
21. Gomes, E. R., Jani, S., and Gundersen, G. G. (2005) *Cell* **121,** 451–463
22. Chrzanowska-Wodnicka, M., and Burridge, K. (1996) *J. Cell Biol.* **133,** 1403–1415
23. Amano, M., Ito, M., Kimura, K., Fukata, Y., Chihara, K., Nakano, T., Matsuura, Y., and Kaibuchi, K. (1996) *J. Biol. Chem.* **271,** 20246–20249
24. Bustelo, X. R. (2000) *Mol. Cell. Biol.* **20,** 1461–1477
25. Turner, M., and Billadeau, D. D. (2002) *Nat. Rev. Immunol.* **2,** 476–486
26. Vicente-Manzanares, M., Ma, X., Adelstein, R. S., and Horwitz, A. R. (2009) *Nat. Rev. Mol. Cell Biol.* **10,** 778–790
27. García-Bernal, D., Parmo-Cabañas, M., Dios-Esponera, A., Samaniego, R., Hernán-P, de la Ossa, D., and Teixidó, J. (2009) *Immunity* **31,** 953–964
28. Tadokoro, S., Shattil, S. J., Eto, K., Tai, V., Liddington, R. C., de Pereda, J. M., Ginsberg, M. H., and Calderwood, D. A. (2003) *Science* **302,** 103–106
29. Yednock, T. A., Cannon, C., Vandevert, C., Goldbach, E. G., Shaw, G., Ellis, D. K., Liaw, C., Fritz, L. C., and Tanner, L. I. (1995) *J. Biol. Chem.* **270,** 28740–28750
30. Schwartz, M. A., and Assoian, R. K. (2001) *J. Cell Sci.* **114,** 2553–2560
31. Go, R. S., and Adjei, A. A. (1999) *J. Clin. Oncol.* **17,** 409–422
32. Wagner, E. F., and Nebreda, A. R. (2009) *Nat. Rev. Cancer* **9,** 537–549
33. Ridley, A. J., Schwartz, M. A., Burridge, K., Firtel, R. A., Ginsberg, M. H., Borisy, G., Parsons, J. T., and Horwitz, A. R. (2003) *Science* **302,** 1704–1709
34. Arthur, W. T., Quilliam, L. A., and Cooper, J. A. (2004) *J. Cell Biol.* **167,** 111–122
35. Lim, J., Dupuy, A. G., Critchley, D. R., and Caron, E. (2010) *J. Cell Biochem.* **111,** 999–1009
36. Assoian, R. K., and Klein, E. A. (2008) *Trends Cell Biol.* **18,** 347–352
37. Montgomery, A. M., Reisfeld, R. A., and Cheresh, D. A. (1994) *Proc. Natl. Acad. Sci. U.S.A.* **91,** 8856–8860
38. Bao, W., and Strömblad, S. (2004) *J. Cell Biol.* **167,** 745–756